Archive of SID

Comparison of the Graft Angles Effects
on the Temporal Wall Shear Stress Gradients
in the Aorto-Coronary and Coronary-Coronary Bypasses

Ahmadlouie Darab, Majid; Ghalichi, Farzan*+

Biomedical and Electrical Faculty, Shahand University of Technology, Tabriz, I.R. IRAN

ABSTRACT: *In this theoretical study, the effect of various types of bypass graft angles on the flow field, has been investigated specially on the temporal Wall Shear Stress (WSS) on the toe, heel and some locations on the bed of the Left Anterior Descending (LAD) artery at the anastomoses areas in the Aorto-Coronary (AC) and Coronary-Coronary (CC) bypasses. Flow fields in both bypasses with angles of 20º, 30º and 40º by 75% stenosis were simulated using Fluent software. The results show high restenosis potential in the side-to-end anastomosis, heel and host artery bed in the CC bypass, and also high restenosis potential at end-to-side in comparing of the AC bypass. Effects of variable graft angles on the WSS on the upper and lower heels in the CC bypass were negligible and the length of the bed influenced by variation of the graft angle was restricted to one diameter distal to the toe in AC bypass and one diameter distal to the lower toe in the CC bypass and finally use of graft angles near 30° was of other important results.*

KEY WORDS: *Wall shear stress, Coronary bypass, Anastomosis and graft angle.*

INTRODUCTION

The use of biological or synthetic grafts to bypass stenosed or occluded arteries is a well established surgical procedure. A large number of vascular bypass grafts have been implanted in patients to revascularize districts downstream from diseased or injured arteries. This surgical technique allows the sites of severe stenoses to be bypassed. In aorto-coronary bypass, natural grafts are anastomosed proximal to the ascending aorta and distal to the coronary artery downstream from the stenosis. However, the development of Intimal Hyperplasia (IH), mostly at the distal anastomosis, can limit the long term success of this procedure. *Hartman et al.* (1976) [1] found that 26 percent of these surgeries fail within 1 year of implantation.

It is fairly well established that the most likely sites of IH are along the suture line, principally at the heel and toe of the anastomosis, and along the floor opposite to the anastomosis. It has postulated that hemodynamic factors, such as unphysiological flow structures and/or wall shear stresses promote IH in the end-to-side anastomosis geometry. *Hofer et al.* (1996) [2], *Bassiouny et al.* (1992) [3], *Moringa et al.* (1985) [4], *Rittgers et al.* (1978) [5] reported that low wall shear stress inserted on the bed in the anastomoses area causes the bed IH. Many investigators showed that high spatial Wall Shear Stress Gradients (WSSG) promote IH (*Lei et al.* (1995) [6], *Kleinstreuer et al.* (1995) [7]) and other authors suggested high temporal gradients of wall shear stress
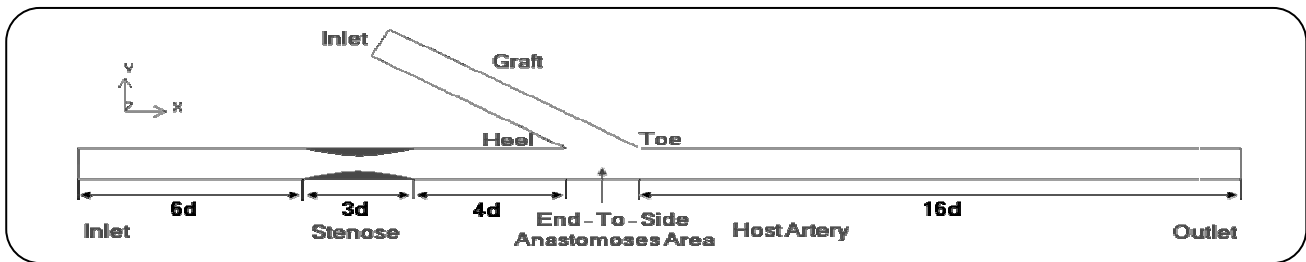
45

Fig. 1: A view of End-to-Side anastomosis and other regions in AC bypass.
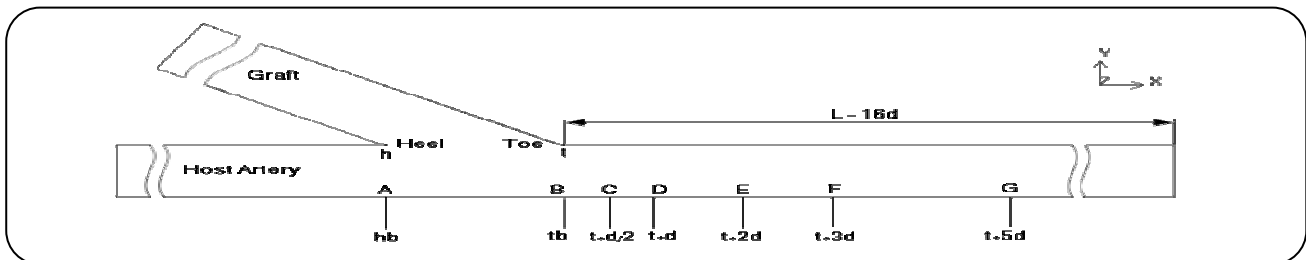

Fig. 2: End-to-Side anastomosis region and points positions on the bed of host artery in the AC bypass.
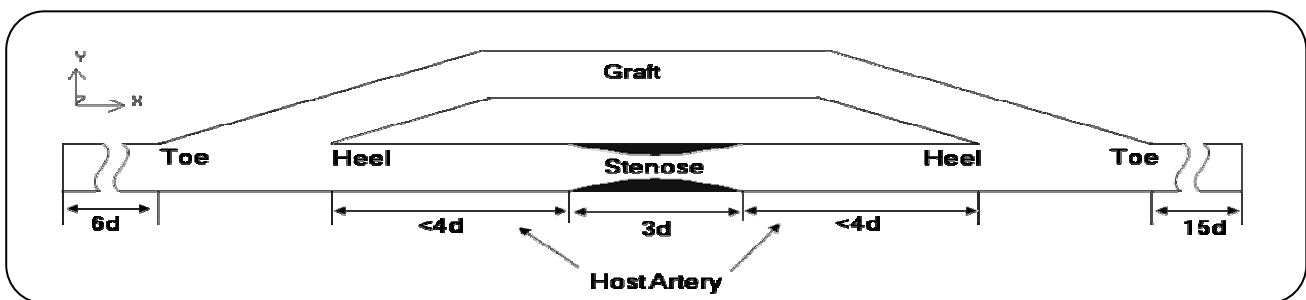

Fig. 3: A view of CC bypass and the lengths of regions.

cause IH proliferation (*Ojha et al.* (1994) [8]). Up to now many investigators worked on these problems numerically or experimentally (*Leuprecht et al.* (2002) [9], *Wentzel et al.* (2000) [10], *Loudon et al.* (1998) [11], *Weston et al.* (1998) [12], *Rindt et al.* (1996) [13]). The overall purpose of this study is to investigate 3D pulsatile blood flow dynamics, numerically specially WSS inserted on toe, heel and some locations on the bed of Left Anterior Descending Artery (LADA) in the regions of the anastomoses in the Aorto-Coronary (AC) and Coronary-Coronary (CC) bypasses by 75% stenosed host artery and $20^°$, $30^°$ and $40^°$ graft angles using Fluent software. Determination of restenosis potential for each bypass and presentation of optimum graft angle are other purposes.

EXPERIMENTAL SECTION

The 3D geometric models of both bypass types (AC, CC) were created by Gambit software. To avoid the influence

of outlet boundary condition on the flow fields in each bypass and to reach fully developed condition at outlet, the host artery was taken sufficiently long. Host and graft arteries have the same diameter (3 mm). The length of the structure for all models is 3 times of artery diameter (3d) (Figs. 1 and 3). In the CC bypass model, the flow inlet is located 6d proximal to the upper toe and in AC; inlet location is 6d proximal to the beginning of stenosis. To indicate any model, we use a name for that such as ac-7530, which shows an AC bypass model with 75% stenoses and 30° graft angle and cc-7530 is referred to a CC bypass by same properties. Some characteristics of bypasses are showed in Table 1. Three CC bypass models and three AC bypass models were prepared [14].

In AC bypass, to study the effects of the variable graft angles on the WSS inserted on the artery bed, 7 points were set on the bed. Point A opposite to the heel, B opposite to the toe and C, D, E, F and G by d/2, d, 2d, 3d and 5d

Table 1: Characteristics of the CC and AC bypass models.

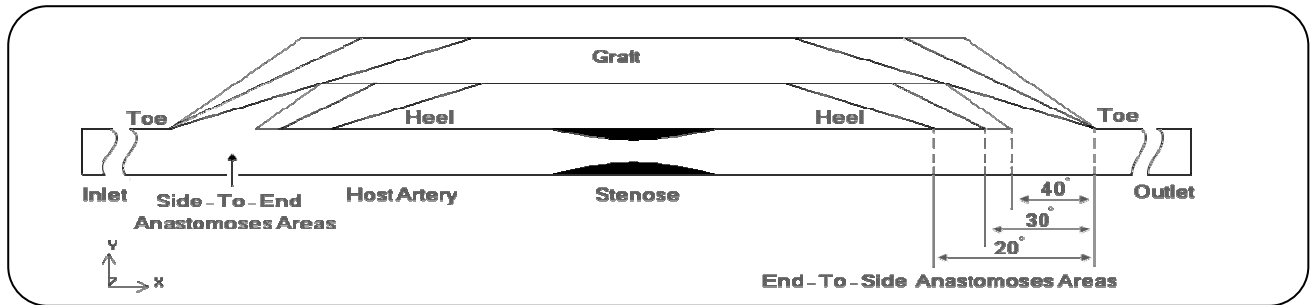| Mesh Number	Graft Angle	Stenos Percent	Artery and Graft Diameter (mm)	Model Name	No.
217364	20	75	3	ac-7520	1
232574	30	75	3	ac-7530	2
233747	40	75	3	ac-7540	3
289666	20	75	3	cc-7520	4
293609	30	75	3	cc-7530	5
317987	40	75	3	cc-7540	6

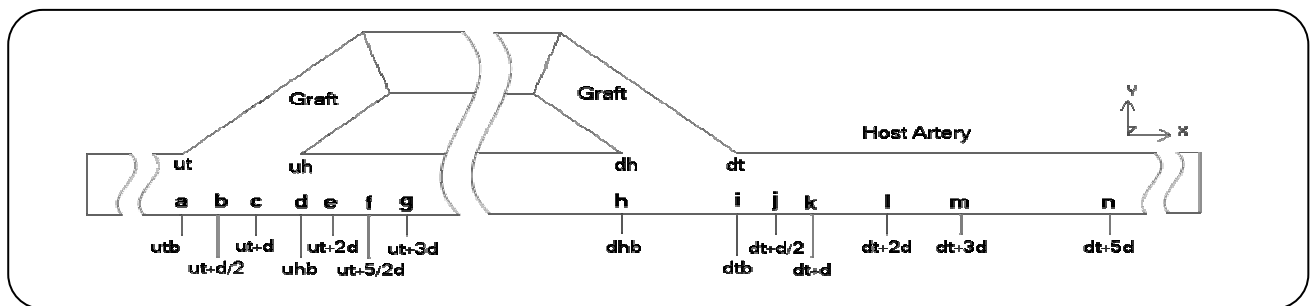*Fig. 4: A schematic of CC bypass and its terminology.*

Fig. 5: Anastomoses regions and points positions on the bed of host artery in the CC bypass.

intervals down to the toe, on the artery bed were selected (Fig. 2). In CC bypass at the side-to-end region 7 points and at the end-to-side region 7 points on the bed of artery were selected: Point a opposite to the upper toe, D opposite to the upper heel and b, c, e, f and g by d/2, d, 2d, 5/2d and 3d intervals down to the up toe, positioned on the bed (Fig. 5). At the end-to-side anastomosis the points h and I are opposite to the down heel and down toe, respectively. The points j, k, l, m and n have d/2, d, 2d, 3d and 5d intervals to the down toe on the bed too. In CC bypass, graft angles in the side-to-end and end-to-side regions were the same. 20°, 30° and 40° angles were used to study the angle effects (Fig.4).

Unstructured tetrahedral and hexahedral meshes were used to grid the both bypass models. Fig. 6 shows the quality of the hexahedral meshes used to mesh the surface of the bypass in the stenosed and anastomosis regions.
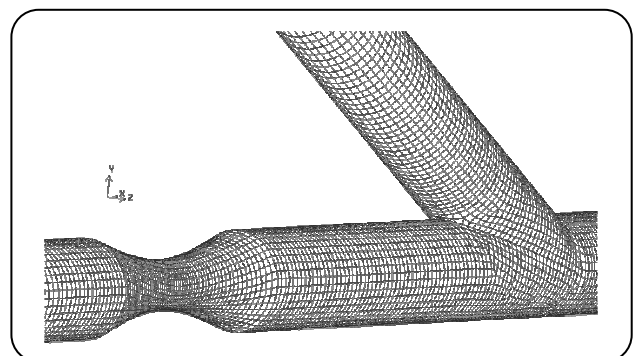

Fig. 6: Mesh quality in Stenosed and anastomosis regions.

THEORITICAL SECTION

Governing equations

The computer simulation is carried out under the assumption of Newtonian and homogenous behavior of blood. Using a viscosity of 3.4 cp and density of 1056 g/L,
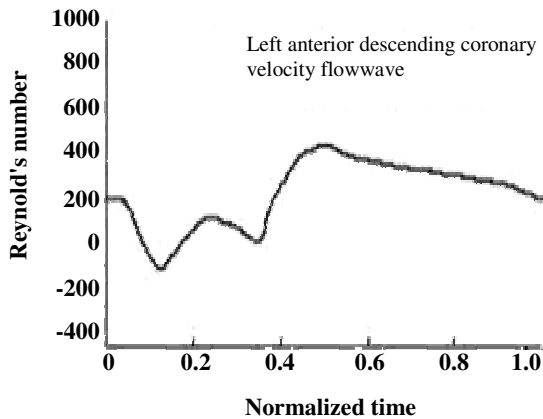
47

Fig. 7: LAD velocity flow wave.

Fig. 8: WSS curves on the ut. Uh, dt, dh in the cc-7530 bypass.

blood flow is 3d, unsteady and incompressible. Artery and graft walls are rigid and impermeable. So the fluid flow is governed by the unsteady, incompressible Navier-Stokes and continuity equations (Eqs. (1) and (2)).

$$\frac{\partial}{\partial t}(\rho u_i) + \frac{\partial}{\partial x_j}(\rho u_i u_j) =$$

$$-\frac{\partial P}{\partial x_i} + \frac{\partial}{\partial x_j}\left[\mu\left(\frac{\partial u_i}{\partial x_j} + \frac{\partial u_j}{\partial x_i} - \frac{2}{3}\delta_{ij}\frac{\partial u_i}{\partial x_i}\right)\right] \quad (1)$$

$$\frac{\partial \rho}{\partial t} + \frac{\partial}{\partial x_i}(\rho u_i) = 0 \quad (2)$$

The governing equations were solved numerically using Fluent® software. The software uses the finite volume method to solve the equations. Because of high L/d ratio and to avoid of divergence of calculations, 3ddp version of this software has been used. Assuming that the heart has 72 bits/min, therefore, the period of a pulse of LAD is 0.8334 second. The LAD flowwave was discretized to 200 time intervals. A Convergence criterion for continuity equation was set to 10^{-5} and a segregated method was applied to the simulation. Three pulses of LAD were considered to reach the steady state in calculations and the results of 3rd pulse presented as final result of this study. The calculation was run in a computer of AMD Sempron(m) Processor 2800+ and 2 giga bytes RAM used. Average simulation time was 36hr (min 34 and max 38).

Boundary conditions

At inlet boundary, the inlet flow is assumed to be perpendicular to the graft and coronary inlets or in the other words at coronary inlet, U_θ and U_r are zero and U_z
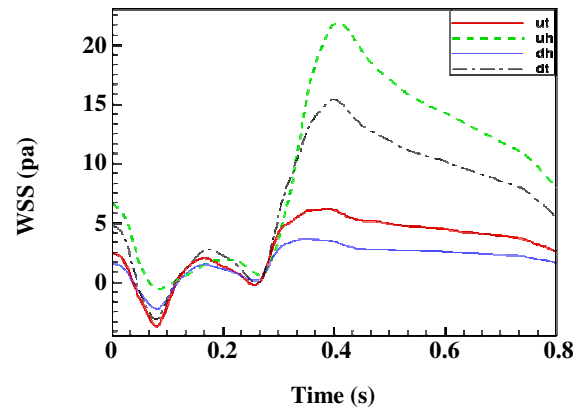
is pulsatile and obeys the LAD velocity flowwave (Eqs. (3) and (4) and Fig. 7). At graft inlet, the tangential velocity is zero and perpendicular velocity obeys from LAD velocity flowwave (Eqs. (5), (6) and Fig. 7).

$$U_r = U_\theta = 0 \quad (3)$$

$$U_z = U_{LAD} \quad (4)$$

$$U_t = 0 \quad (5)$$

$$U_n = U_{LAD} \quad (6)$$

RESULTS AND DISCCUSION

One of the important purposes of this study was to compare the WS and WSSG inserted on the sites promoting to restenosis such as the toe, the heel and the bed of the host artery in the anastomoses regions in the CC and AC bypasses. Finally, we have determined the restenosis potential in the anastomoses areas for the both bypass types. Presenting the optimum graft angle and the bypass by patency rate are of other purposes.

• In the CC bypass for angle of 30º the WSS on the upper heel (uh) is higher than that inserted on the lower toe and heel (dh, dt) and upper toe too (Fig. 8).

• By increasing the angle, WSS on the upper heel and lower toe increase and for 40°, WSS on the lower toe is greater than WSS on the upper heel (Figs. 8 to 9).

• Variation of the graft angles has negligible effects on the WSS on the upper heel in the CC bypass (Figs. 8 to 9).

• The WSS on the lower heel has the lowest amount and the variation of the graft angles has negligible effect on that (Figs. 8 to 9).
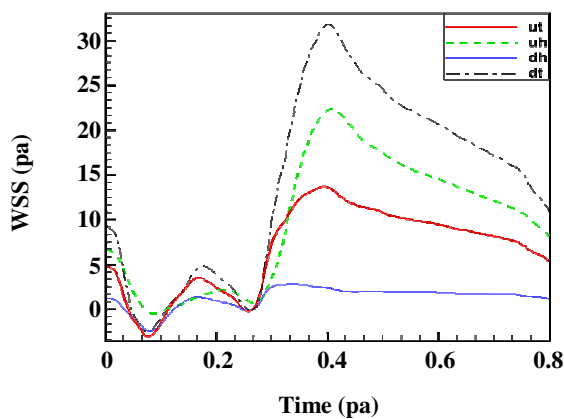
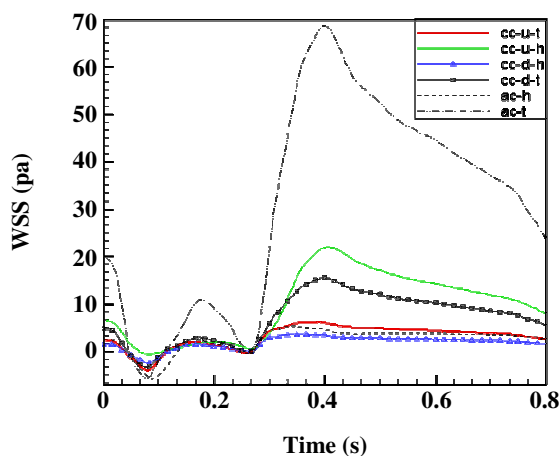**Fig. 9: WSS curves on the ut, uh, dt, dh in the cc-7540 bypass.**

Fig. 10: WSS curves on the ut, uh, dt, dh in the cc-7530 and h, t in the ac-7530 bypasses.

• The WSS on the upper heel is greater than on the upper toe, but in the end-to-side region it is vice versa (Figs. 8 to 9).

• Increasing the graft angle causes the WSS on the lowewr toe to increase (Figs. 8 to 9).

• The WSS on the heel in the AC bypass is greater than the lower heel in the CC bypass, but it is less than upper heel and all of the toes in both bypass types (Figs. 8 to 9).

• The WSS on the lower toe is high and by increasing the graft angle, it becomes greater than WSS on the upper heel (Figs. 8 to 9).

• For all of the graft angles the WSS on the toe in the AC bypass (ac-t) is greater than both upper and lower toe (cc-ut, cc-dt) in CC bypass (Figs. 10 and 11).

• Temporal WSSG on the toe in the AC bypass is greater than all toes and heels in the CC bypass, and

also it is greater than the WSS on the heel in the AC bypass (ac-h) (Figs. 10 and 11).

• For all of the graft angles the WSS on the lower heel in the CC bypass, in comparison with both the lower and the upper toe and the upper heel in the CC bypass and also in comparison with the toe and heel of the AC bypass, is low and it has very low value (Figs. 10 and 11).

• Increasing the graft angle causes the WSS to decrease on the heel in the AC bypass until $40^{°}$ of the graft angle at which the WSS is very negligible (Figs. 10 and 11).

• Increasing the graft angle from 20° to 30° causes the decrease of the WSS on the up toe, but from 30° to 40° it becomes reverse (Figs. 10 and 11).

• In the AC bypass, increasing the graft angle causes the decrease of the WSS on the heel (Figs. 11 to 13).

• In the AC bypass, WSS on the toe is higher than other susceptible sites to restenosis and WSS on the toe is higher too (Figs. 10 and 11).

• In the AC bypass, WSS on the bed, opposite to the heel (A) in comparison with other points is the lowest, but on the contrary, WSS on the bed opposite to the toe (B) is higher than other points on the bed and it's WSSG is the highest too (Figs. 12 and 13).

• In the AC bypass, the WSS on the bed decreased by increasing the distance from the toe and moving to the distal to the toe (Figs. 12 and 13).

• In spite of the increasing of the graft angle that causes to increase the WSS on the bed of artery opposite to the toe (between points B and C), but the variation of the graft angle doesn't have effect on the WSS inserted on the bed in the distal regions to the toe and it's effective extent is utmost 1d distal to the toe (Figs. 12 and 13).

• In the CC bypass, WSS on the bed opposite to the upper toe (point a) in comparison with the other points on the bed in the side-to-end anastomosis, is high and has the highest WSSG (Figs. 14 and 15).

• In the CC bypass, WSS on the bed decreases moving distal to the upper toe and generally WSS on the artery bed at side-to-end region, between heel and stenosis is the lowest (Figs. 14 and 15).

• In the CC bypass, moving to the distal regions of the end-to-side anastomosis, the WSS on the bed decreases as well as side-to-end anastomosis (Figs. 16 and 17).

• In the CC bypass, for all of the graft angles WSS on the point j (d/2 distal to the down toe) is greater than the other points on the artery bed (Figs. 16 and 17).
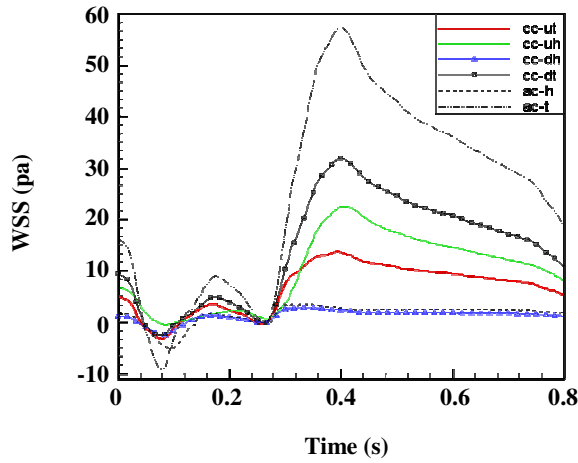
49

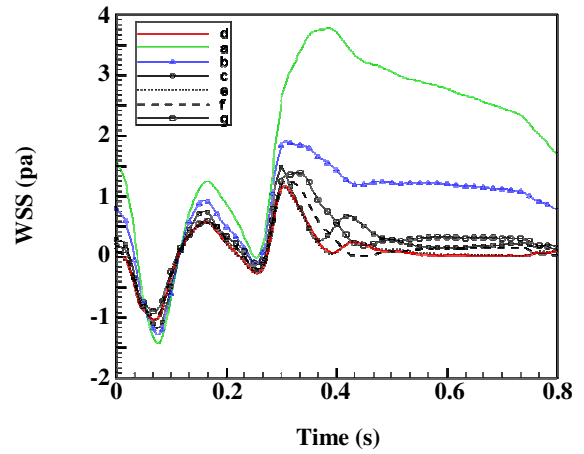*Fig. 11: WSS curves on the ut, uh, dt, dh in the cc-7540 and h, t in the ac-7540 bypasses.*

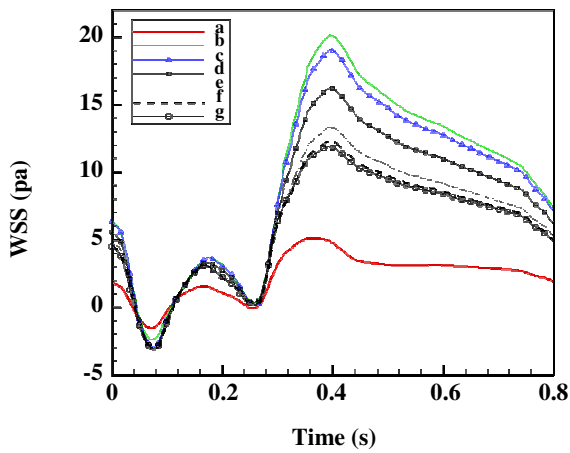*Fig. 14: WSS curves on the points a, b, c, d, e, f and g in the cc-7530 bypass.*

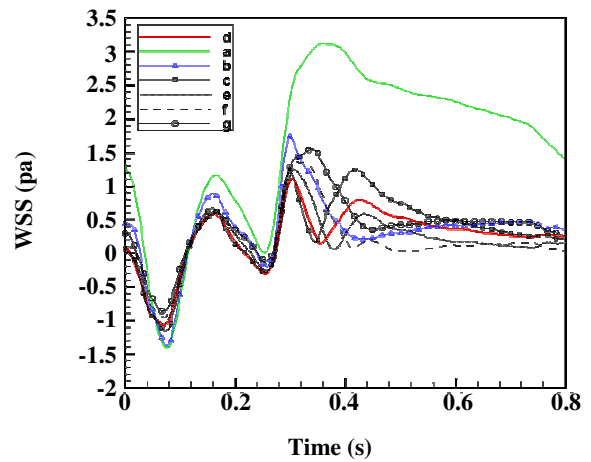*Fig. 12: WSS curves on the points a, b, c, d, e, f and g in the ac-7530 bypass.*

Fig. 15: WSS curves on the points a, b, c, d, e, f and g in the cc-7540 bypass.

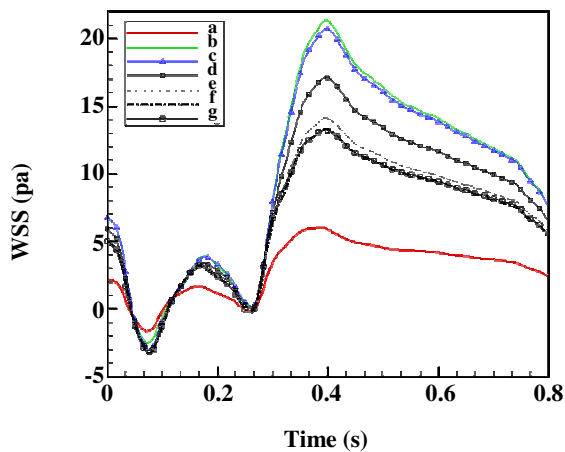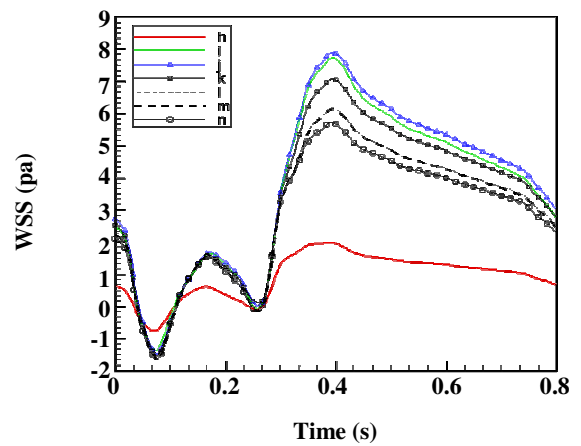*Fig. 13: WSS curves on the points a, b, c, d, e, f and g in the ac-7540 bypass.*

Fig. 16: WSS curves on the points h, i, j, k, l, m and n in the cc-7530 bypass.
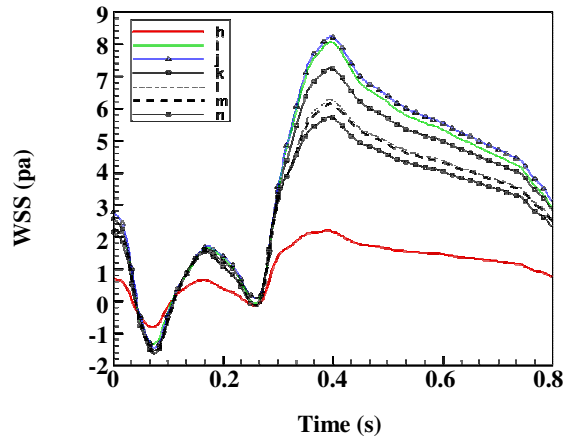
Archive of SID

Fig. 17: WSS curves on the points h, i, j, k, l, m and n in the cc-7540 bypass.

• In the CC bypass, variation of the graft angle in the WSS on the bed in the region distal to the end-to-side anastomosis has negligible effects and its effectivness is limited to 1d distal to the lower toe (Figs. 16 and 17).

CONCLUSIONS

According to *Giddens et al.* (1990) [15] results, we have recognized that the critical value for WSS inserted on the variable locations of the LAD artery is 15 (Pa), then in the any region if the WSS is lower than critical WSS, that site is susceptible to the restenosis. So according to the results of this study, the restenosis potential in the side-to-end anastomosis in the CC bypass is high and branching of the flow and existence of the stenosis are of the major reasons. On the other hand, restenosis potential in the end-to-side region in the CC bypass is higher than similar region in the AC bypass. In the AC bypass the restenosis potential in the regions proximal to the stenosis and distal to the heel is high and the decreasing the graft angle decreases this potential. Also we should note that the temporal WSS on the distal regions to the anastomosis in the AC bypass in comparison with the CC bypass is high, but lowering the graft angle decreases this potential so generally we offer AC bypass as the bypass with high patency rate and angles near 30º as optimum bypass angles.

REFERENCES

[1] Hartman C. W., Kong Y., et al., Aortocoronary Bypass Surgery: Correlation of Angiographic, Symptomatic and Functional Improvement at 1 Year, *Am. J. Cardiol.*, **37**, p. 352 (1976).

[2] Hofer M., Rappitsch G., Perktold K., Tuble W., Schima H., Numerical Study of Wall Mechanics and Fluid Dynamics in End-to-Side Anastomoses and Correlation to Intimal Hyperplasia, *J. Biomechanics* **29**, p. 1297 (1996).

[3] Bassiouny H.S., White S.,Glagov S.,Choi E., Giddens D.P., Zarins C. K., Anastomotic Intimal Hyperplasia: Mechanical Injury or Flow Induced, *J. Vascular Surgery*, **15,** p. 708-717 (1992).

[4] Moringa K., Okadome K., Kuoki M., Miyazaki T., Muto Y., Inokuchi K., Effect of Arterially Transported Autogenous Vein in Dogs, *J. Vascular Surgery*, **2**, p. 430 (1985).

[5] Rittgers S. E., Karayannacos P. E., Guy J. F., Velocity Distribution and Intimal Proliferation in Autologous Vein Grafts in Dogs, *Circulation Research*, **42**, p. 792 (1978).

[6] Lei M., Kleinstreuer C., Trusky G., Numerical Analysis and Prediction of Atherogenic Sites in Branching Arteries, ASME J., *Biomechanical Engineering*, **117**, p. 350 (1995).

[7] Kleinstreuer C., Lei M., Buchanan J., Archie J., Hemodynamics of Femoral Graft-Artery Connector Mitigating Restenosis, In: Hull M. (Ed.), *Proceedings of the 1995 Bioengineering Conference*, BED- Vol. 31, ASME Press, New York, p. 171-172 (1995).

[8] Ojha M., Wall Shear Stress Temporal Gradient and Anastomotic Intimal Hyperplasia, *Circulation Research*, **7**, p. 1227 (1994).

[9] Leuprecht A. et al., Numerical Study of Hemodynamics and Wall Mechanics in Distal End-to-Side Anastomoses of Bypass Grafts, *J. Biomechanics*, **35**, p. 225 (2002).

[10] Wentzel J. J., et al., Coronary Stent Implantation Changes 3-D Vessel Geometry and 3-D Shear Stress Distribution, *J. Biomechanics*, **33**(10), p. 1287 (2000).

[11] Loudon C., et al., The Use of the Dimensionless Womersley Number to Characterize the Unsteady Nature of Internal Flow, *J. Theor. Biol.*, **191** (**1**), p. 63 (1998).

51

[12] Weston S.J. et al., Combined MRI and CFD Analysis of Fully Developed Steady and Pulsatile Laminar Flow through a Bend, J. *Magn. Reson. Imaging*, **8** (**5**), p. 1158 (1998).

[13] Rindt C. C., and Steenhoven A. A., Unsteady Flow in a 3-D Model of the Carotid Artery Bifurcation, *J. Biomechanical Eng.*, **118**(1), p. 90 (1996).

[14] Ahmadlouie darab M., Simulation of Pulsatile Blood Flow in the Bypassed Coronary Arteries and study the Restenosis Reasons, MSc Thesis, Biomed. Group, Chem. Eng. Dep., Sharif University of Technology, Tehran, Iran, Mar., (2004).

[15] Giddens D.P., Zarins C.K., Glogov S., Response of Arteries near Wall Fluid Dynamic Behavior, *Appl. Mech. Rev.*, **43**, p. 98 (1990).